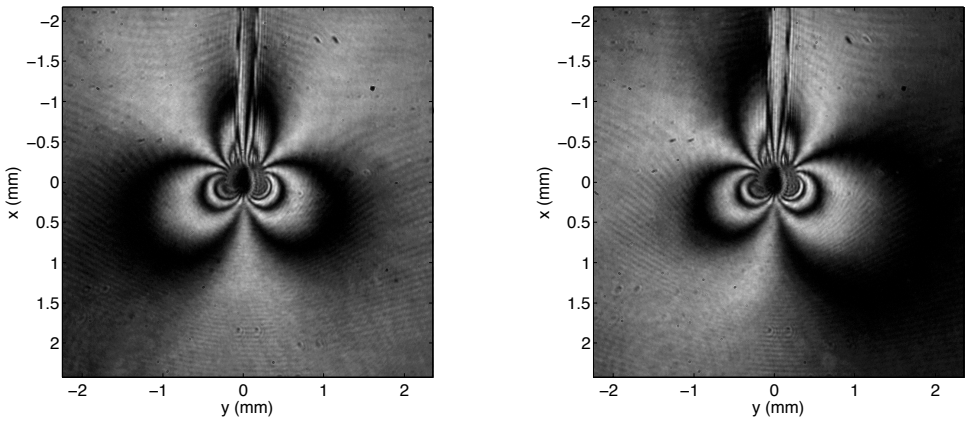

(a) I_1^{Ex} (b) I_2^{Ex}

(c) I_3^{Ex} (d) I_4^{Ex}

Figure 4.11: Experimental phase-shifted images from horizontal shearing CGS using pure $E_x\hat{\imath}$ input for specimen HomC1 for $K_I = 0.514$ MPa$\sqrt{\text{m}}$ and $K_{II} = 4.4$ kPa$\sqrt{\text{m}}$

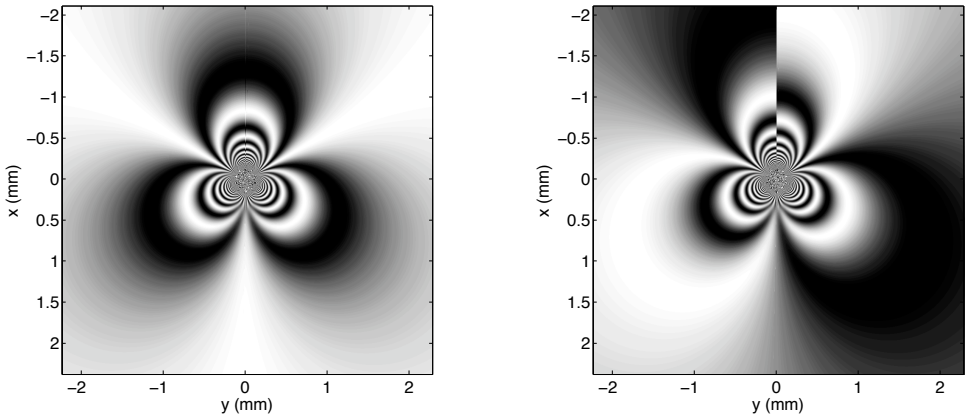

(a) I_1^{Ex} (b) I_2^{Ex}

(c) I_3^{Ex} (d) I_4^{Ex}

Figure 4.12: Theoretical phase-shifted images from horizontal shearing CGS using pure $E_x\hat{\imath}$ input for specimen HomC1 for $K_I = 0.514$ MPa$\sqrt{\text{m}}$ and $K_{II} = 4.4$ kPa$\sqrt{\text{m}}$

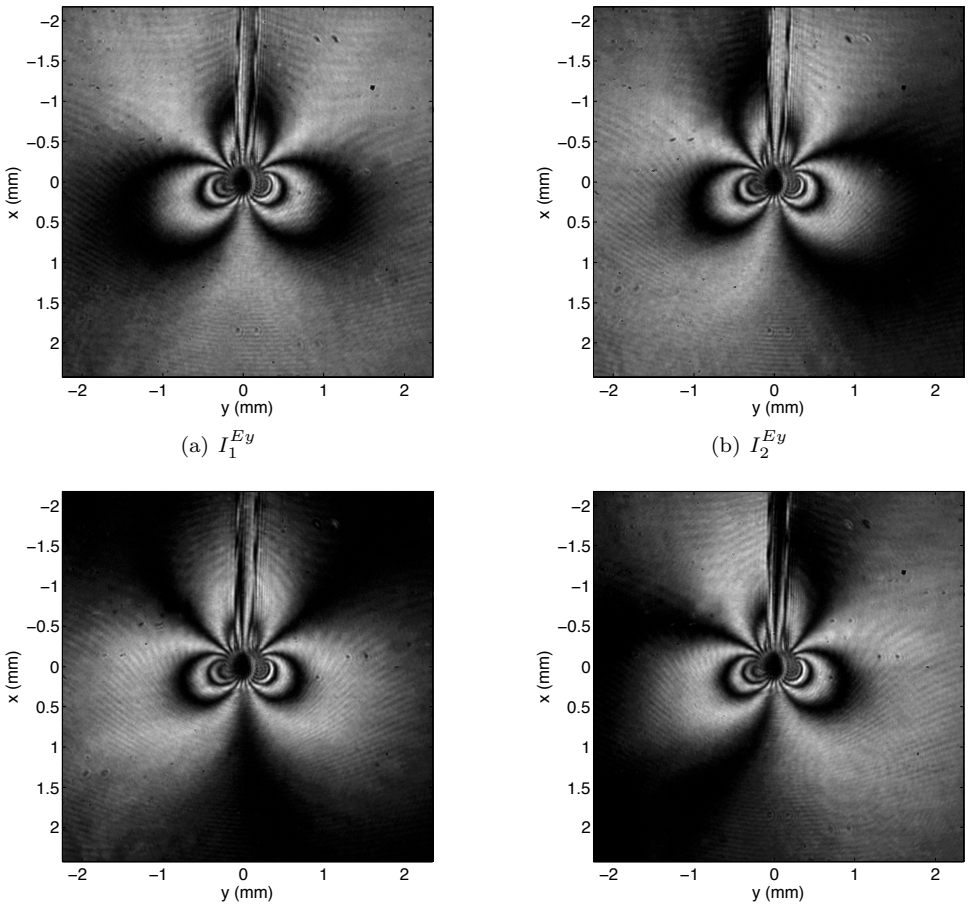

(a) I_1^{Ey} (b) I_2^{Ey}

(c) I_3^{Ey} (d) I_4^{Ey}

Figure 4.13: Experimental phase-shifted images from horizontal shearing CGS using pure $E_y\hat{j}$ input for specimen HomC1 for $K_I = 0.514$ MPa$\sqrt{\text{m}}$ and $K_{II} = 4.4$ kPa$\sqrt{\text{m}}$

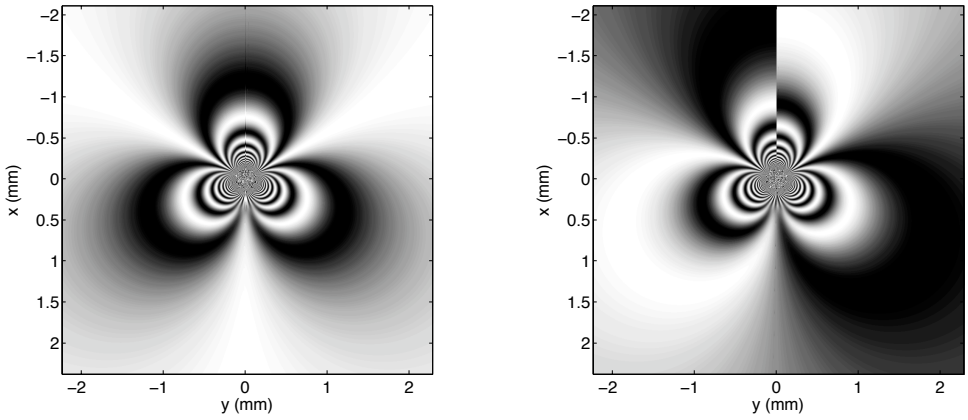

(a) I_1^{Ey} (b) I_2^{Ey}

(c) I_3^{Ey} (d) I_4^{Ey}

Figure 4.14: Theoretical phase-shifted images from horizontal shearing CGS using pure $E_y\hat{\jmath}$ input for specimen HomC1 for $K_I = 0.514$ MPa$\sqrt{\text{m}}$ and $K_{II} = 4.4$ kPa$\sqrt{\text{m}}$

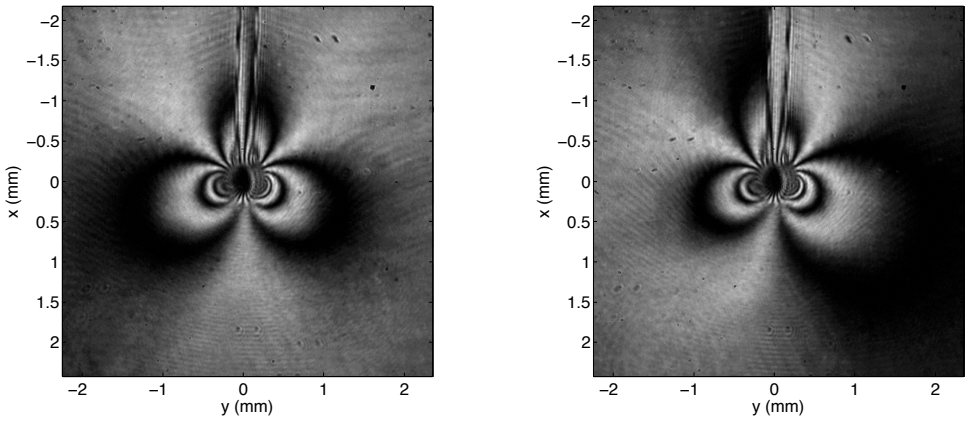

(a) I_1^{circ} (b) I_2^{circ}

(c) I_3^{circ} (d) I_4^{circ}

Figure 4.15: Experimental phase-shifted images from horizontal shearing CGS using the $\lambda/4$ polarization method for specimen HomC1 for $K_I = 0.514$ MPa$\sqrt{\text{m}}$ and $K_{II} = 4.4$ kPa$\sqrt{\text{m}}$

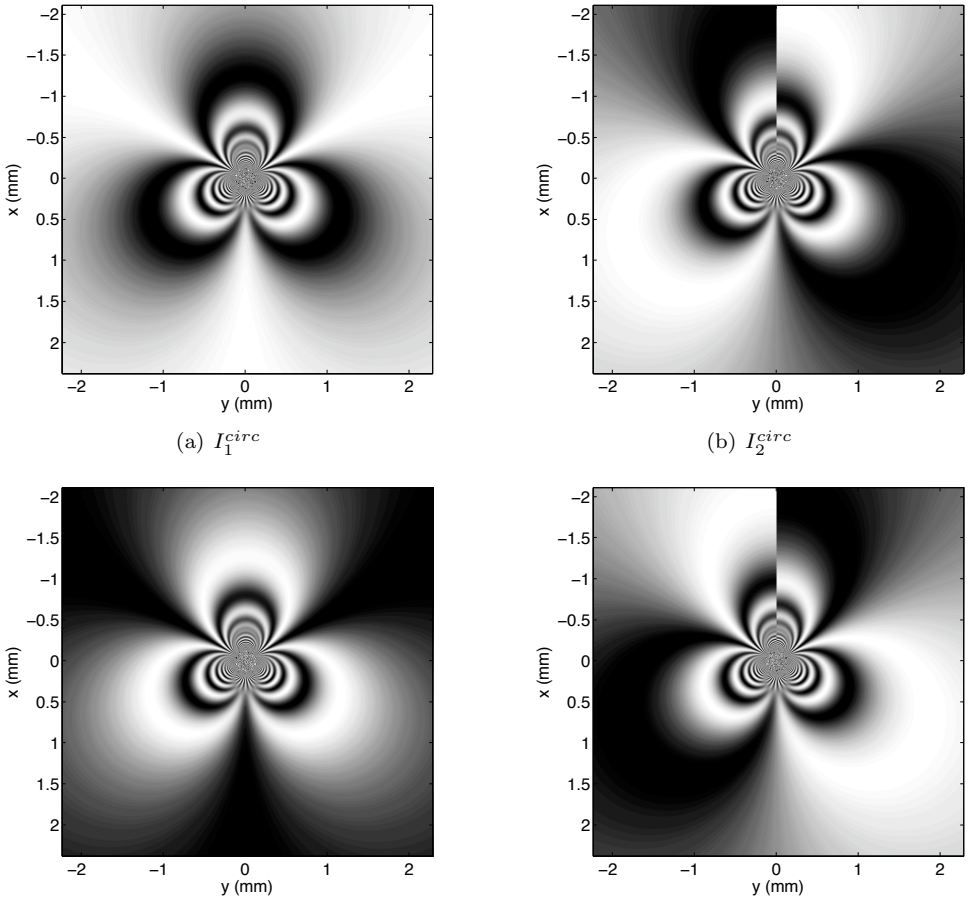

(a) I_1^{circ} (b) I_2^{circ}

(c) I_3^{circ} (d) I_4^{circ}

Figure 4.16: Theoretical phase-shifted images from horizontal shearing CGS using the $\lambda/4$ polarization method for specimen HomC1 for $K_I = 0.514$ MPa$\sqrt{\text{m}}$ and $K_{II} = 4.4$ kPa$\sqrt{\text{m}}$